

# On the persistence of breathers at deep water

F. Fedele<sup>1)</sup>

School of Civil and Environmental Engineering,  
School of Electrical and Computer Engineering,  
Georgia Institute of Technology, GA 30332 Atlanta, USA

Submitted 27 August 2013

Resubmitted 23 September 2013

The long-time behavior of a perturbation to a uniform wavetrain of the compact Zakharov equation is studied near the modulational instability threshold. A multiple-scale analysis reveals that the perturbation evolves in accord with a focusing nonlinear Schrodinger equation for values of wave steepness  $\mu < \mu_1 \approx 0.274$ . The long-time dynamics is characterized by interacting breathers, homoclinic orbits to an unstable wavetrain. The associated Benjamin–Feir index is a decreasing function of  $\mu$ , and it vanishes at  $\mu_1$ . Above this threshold, the perturbation dynamics is of defocusing type and breathers are suppressed. Thus, homoclinic orbits persist only for small values of wave steepness  $\mu \ll \mu_1$ , in agreement with recent experimental and numerical observations of breathers.

DOI: 10.7868/S0370274X13210029

**1. Introduction.** The dynamics of unidirectional and inviscid narrowband waves in deep water obeys the one-dimensional (1D) nonlinear Schrodinger (NLS) equation. In accord with this model, a finite-amplitude uniform wavetrain is unstable to infinitesimal subharmonic disturbances, the so-called modulational or Benjamin–Feir instability [1, 2]. The long-time behavior of an unstable wavetrain is characterized by successive modulation and demodulation cycles [3, 4], or Fermi–Pasta–Ulam (FPU) recurrence [5]. This is the signature of breathers, homoclinic orbits to an unstable uniform wavetrain [6].

Recent studies propose the NLS breather as a model to explain rogue waves, unusually large waves that appear from nowhere at the ocean [6–11]. Breathers have been observed in laboratory experiments at sufficiently small values of the carrier wave steepness  $\sim 0.01$ – $0.09$  [12, 13], and in agreement with numerical simulations of the fully nonlinear Euler equations [14]. However, recent experimental results on the Peregrine breather indicate that breathers are suppressed somewhat as wave steepness increases [15].

In this work, we propose to further investigate the modulational properties of unidirectional deep-water wavetrains and the persistence of breathers. We aim to study the weakly nonlinear space-time evolution of a linearly unstable wavetrain of the compact Zakharov equation recently derived by [16], hereafter referred to as cDZ.

The paper is organized as follows. In section 2, we introduce the cDZ equation and derive the associated set of equations in terms of local amplitude and phase of the wave field. In section 3, the linear stability analysis of a uniform wavetrain is presented. This is followed in section 4 by a multiple-scale analysis of the perturbation dynamics near the modulation instability threshold. Concluding remarks on the theoretical results are finally presented.

**2. Governing equations.** We consider the local form of the cDZ equation and ignore wave-induced current effects. Define  $k_0 = \omega_0^2/g$  and  $\omega_0$  as the wavenumber and frequency of the carrier wave  $e^{i(k_0x - \omega_0t)}$ , and  $c_g$  is the associated group velocity in deep water. Drawing upon [17], the leading order wave surface  $\eta$  is given by

$$k_0\eta(X, T) = B(X, T)e^{i(k_0x - \omega_0t)} + \text{c.c.}, \quad (1)$$

where the non-dimensional envelope  $B$  evolves on the scales  $X = k_0(x - c_g t)$  and  $T = \omega_0 t$  in accord with

$$i\partial_T B = \frac{\delta\mathcal{H}}{\delta B^*}. \quad (2)$$

Here,  $\delta$  denotes variational differentiation, the Hamiltonian is given by

$$\mathcal{H} = \int_{\mathbb{R}} \left[ B^* \Omega B + \frac{i}{4} |SB|^2 [B(SB)^* - B^* SB] \right] dX, \quad (3)$$

and

$$S = \partial_X + i, \quad \Omega = \frac{1}{8} \partial_{XX},$$

where third- and higher-order dispersion terms are not accounted for. The carrier wave steepness  $\mu = k_0 a_0 = 2|B|$ , with  $a_0 = 2|B|/k_0$  as the amplitude of  $\eta$ . Note

<sup>1)</sup>e-mail: fedele@gatech.edu

that (2) is valid if  $k_0 \gg 1$  or if the spectrum of  $B$  has negligible energy for wavenumbers  $k < -k_0$ , viz. the spectral bandwidth  $\Delta k/k_0 < 1$ . Otherwise, a projection operator  $P^+$  must be applied to the nonlinear term of (2) in order to nullify Fourier components of  $B$  with wavenumbers  $k < -k_0$ . In the following, we assume that the above conditions are met and  $P^+$  is neglected.

We aim to study the long-time evolution of a perturbation to the uniform wavetrain solution  $B_0$  of (2), namely

$$B_0(T) = \sqrt{E_0} e^{-iE_0 T}, \quad (4)$$

where  $E_0$  is the squared amplitude of the wavetrain. To do so, we define

$$B = \sqrt{E(X, T)} e^{i\phi(X, T) - iE_0 T}, \quad (5)$$

with  $E$  as the squared envelope amplitude and  $\phi$  the respective phase. The Lagrangian  $\mathcal{L}$

$$\mathcal{L} = \frac{i}{2} (B^* \partial_T B - \partial_T B^* B) - \mathcal{H} \quad (6)$$

associated with (2) simplifies to

$$\begin{aligned} \mathcal{L} = & -E(E_0 + \phi_T) - \\ & - \frac{1}{32E} \left\{ +E_X^2 [-1 + 4E(1 + \phi_X)] + \right. \\ & \left. + 4E^2 [-\phi_X^2 + 4E(1 + \phi_X)^3] \right\}, \quad (7) \end{aligned}$$

where subscripts denote partial derivatives with respect to  $T$  or  $X$ . The dynamical equations for  $E$  and  $\phi$  follow by variational differentiation of  $\mathcal{L}$  as

$$\begin{cases} \partial_T \phi + \omega = 0, \\ \partial_T E + \partial_X (VE) = 0, \end{cases} \quad (8)$$

where the local frequency of the wavetrain

$$\begin{aligned} \omega = & \frac{\partial \mathcal{H}}{\partial E} - \partial_X \left( \frac{\partial \mathcal{H}}{\partial E_X} \right) = \\ = & \frac{E_{XX}}{16E} [1 - 4E(1 + \phi_X)] + \\ - & \frac{1}{32} \left( \frac{E_X}{E} \right)^2 - \frac{\phi_X^2}{8} + E(1 + \phi_X)^3 - E_0 - \frac{1}{4} E_X \phi_X, \quad (9) \end{aligned}$$

and the respective energy flux velocity

$$\begin{aligned} V = & \frac{1}{E} \frac{\partial \mathcal{H}}{\partial \phi_X} = \\ = & -\frac{\phi_X}{4} (1 - 12E) + \frac{3}{2} E + \frac{1}{8} \left( \frac{E_X^2}{E} + 12E \phi_X^2 \right). \quad (10) \end{aligned}$$

Note that the NLS model studied in [3] is recovered if cubic terms in (8) are neglected. The uniform wavetrain solution (4) written in terms of  $E$  and  $\phi$  is given by

$$\mathbf{v}_0 = \begin{bmatrix} E_0 \\ 0 \end{bmatrix}.$$

In the following we will study the linear stability of  $\mathbf{v}_0$  to infinitesimal perturbations in accord with the dynamical equations (8).

**3. Linear stability analysis.** Given a small parameter  $\epsilon$ , perturb  $\mathbf{v}_0$  as

$$\mathbf{v} = \mathbf{v}_0 + \epsilon \mathbf{v}_1, \quad (11)$$

where

$$\mathbf{v}_1 = \begin{bmatrix} E_1(X, T) \\ \phi_1(X, T) \end{bmatrix}.$$

From (8), the perturbation  $\mathbf{v}_1$  satisfies the linearized vector equation

$$\partial_T \mathbf{v}_1 + \mathcal{M}_0 \mathbf{v}_1 = 0, \quad (12)$$

where

$$\mathcal{M}_0 = \begin{bmatrix} 3E_0 \partial_X & \frac{-E_0(1 - 12E_0)}{4} \partial_{XX} \\ 1 + \frac{1 - 4E_0}{16E_0} \partial_{XX} & 3E_0 \partial_X \end{bmatrix}. \quad (13)$$

The harmonic solution of (12) is

$$\mathbf{v}_1 = \begin{bmatrix} A e^{i(kX - wT)} + \text{c.c.} \\ \phi_0 \end{bmatrix}, \quad (14)$$

where  $A$  and  $\phi_0$  are constant parameters, and the wavenumber  $k$  and frequency  $w$  satisfy

$$\begin{aligned} w^2 - 6E_0 k w + \frac{E_0 k^2}{4} - \frac{k^4}{64} + \\ + E_0 k^2 \left( 6E_0 + \frac{k^2}{4} \right) - \frac{3}{4} E_0^2 k^4 = 0. \quad (15) \end{aligned}$$

The growth rate  $\gamma$  follows from the imaginary part of  $w$  as

$$\gamma^2 = -\frac{\Delta}{4} = \frac{1}{64} (1 - 3\mu^2) k^2 [4\mu^2 - (1 - \mu^2) k^2], \quad (16)$$

where the carrier wave steepness  $\mu = 2\sqrt{E_0}$  and  $\Delta$  is the discriminant of the quadratic equation (15). Note that  $\gamma$  vanishes at the critical dimensionless wavenumber  $k_c$  defined by

$$k_c^2 = \frac{16E_0}{1 - 4E_0} = \frac{4\mu^2}{1 - \mu^2}, \quad (17)$$

and the respective frequency  $w_c = 3E_0 k_c$ . Near the instability threshold  $k_c$ , the cDZ equation (2) is valid if  $k_c^2 < 1$  in order to have Fourier components of  $\eta$  with nonnegative wavenumbers only. This yields the upper bound  $\mu_m = 0.447$  for  $\mu$ , which is nearly the same as the Stokes limiting steepness 0.448.

Thus, for  $\mu < \mu_m$ , perturbations with  $k < k_c$  are unstable (subharmonic instability). For  $\mu \geq \mu_m$ , the cDZ is beyond the range of its validity. Nonetheless, the linear analysis predicts that modulational (subharmonic) instability disappears at  $\mu_c = \sqrt{1/3} \approx 0.577$ . Note that the same threshold holds if non-local effects are retained in the linear stability analysis [16]. For  $\mu > \mu_c$ , superharmonic instability appears in agreement with the stability analysis in [18] for the original Zakharov (Z) equation, which yields  $\mu_c \approx 0.5$ . Here, the two thresholds are slightly different because the cDZ and Z equations are given in terms of different canonical variables.

**4. Long-time evolution of an unstable wavetrain.** Near the modulation instability threshold  $k_c$ , wave dynamics can be determined by means of multiple-scale perturbation methods. In particular, for the NLS equation the time analysis in [3] revealed that the long-time behavior of an unstable wavetrain evolves to a periodic state exhibiting FPU recurrence. Hereafter, we extend this analysis to the cdZ equations (8). Introduce the independent multiple scales  $\xi = \epsilon^2 X$ ,  $\tau = \epsilon T$  and consider the ordered expansion for  $E$  and  $\phi$  in the small parameter  $\epsilon$

$$\mathbf{v} = \mathbf{v}_0 + \epsilon \mathbf{v}_1 + \epsilon^2 \mathbf{v}_2 + \epsilon^3 \mathbf{v}_3 + \dots, \quad (18)$$

where

$$\mathbf{v}_0 = \begin{bmatrix} E_0 \\ 0 \end{bmatrix}, \quad \mathbf{v}_j = \begin{bmatrix} E_j(X, T, \xi, \tau) \\ \phi_j(X, T, \xi, \tau) \end{bmatrix}.$$

To ensure instability, the perturbation wavenumber  $k$  is set just below the critical threshold  $k_c$ , i.e.  $k = k_c - \epsilon^2 q_e$ , where the parameter  $q_e > 0$  is arbitrary and of  $O(1)$ . The corresponding growth rate is of  $O(\epsilon)$  and follows from (16) as

$$\bar{\gamma} = \epsilon \sqrt{\chi q_e}, \quad \chi = \frac{E_0 k_c (1 - 12E_0)}{2} = \frac{\mu^3 (1 - 3\mu^2)}{4\sqrt{1 - \mu^2}}.$$

Note that  $\bar{\gamma} > 0$  for  $\mu < \mu_c$ , indicating linear instability (see Fig. 1). To  $O(\epsilon)$ , the asymptotic solution for  $\mathbf{v}$  is given by

$$\mathbf{v} = \begin{bmatrix} E_0 + \epsilon A(\xi, \tau) e^{i\theta} + c.c. \\ \epsilon \phi_0(\xi, \tau) \end{bmatrix} + O(\epsilon^2),$$

where  $\theta = k_c X - w_c T$ , and the perturbation amplitude  $A$  evolves on the slow scales  $\xi$  and  $\tau$  in accord with the NLS equation (the linear term can be removed by the canonical transformation  $A \rightarrow A e^{iq_e \xi}$ )

$$i\chi A_\xi = A_{\tau\tau} + \beta |A|^2 A - \chi q_e A, \quad (19)$$

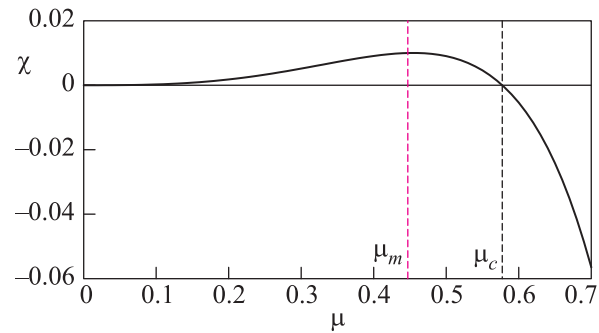


Fig. 1. Coefficient  $\chi$  as function of the carrier wave steepness ( $\mu_m \approx 0.447$ ,  $\mu_c \approx 0.577$ )

where

$$\beta = \frac{2(1 - 2\mu^2)(1 - 14\mu^2 + 8\mu^4)}{(1 - \mu^2)^3} = 2 - 26\mu^2 + O(\mu^3).$$

This stems from removing the secularities of the  $O(\epsilon^3)$  equation for  $\mathbf{v}_3$  in the multiple-scale hierarchy [19]. The phase  $\phi_0$  depends upon  $A$  and given by

$$\phi_0(\xi, \tau) = \phi_0(\xi, \tau = 0) - \int_0^\tau \frac{k_c^2}{16E_0^2} |A(\xi, s)|^2 ds.$$

Neglecting spatial variability, (19) simplifies to

$$A_{\tau\tau} + \beta |A|^2 A - \chi q_e A = 0,$$

in agreement with [3]. This can be interpreted as the equation of motion of a particle in a potential well

$$V(|A|) = -\frac{1}{2} \chi q_e |A|^2 + \frac{1}{4} \beta |A|^4.$$

Clearly, if nonlinearities are neglected ( $\beta = 0$ ), the particle motion is unstable since  $\chi q_e > 0$  whereas, for  $\beta > 0$  periodic solutions exist in terms of Jacobi elliptic functions.

The Benjamin–Feir Index (BFI) associated with the NLS equation (19) is proportional to  $\beta$  [9] and it measures the likelihood of occurrence of breathers. In particular,  $\beta$  decreases as  $\mu$  increases and it vanishes at  $\mu_1 \approx 0.274$ , as clearly illustrated in Fig. 2. For  $\mu < \mu_1$ , the NLS equation (19) is of focusing type since  $\beta > 0$ , and the perturbation  $A$  evolves to a state dominated by breathers. However, their amplitude and likelihood of occurrence diminish somewhat as  $\mu$  increases because the BFI vanishes at  $\mu_1$ . Thus, homoclinic orbits persist for  $\mu \ll \mu_1$  in agreement with the Melnikov analysis applied to the higher-order NLS (HONLS) equation in [20], and the recent experimental and numerical observations of higher-order breathers at sufficiently small values of wave steepness  $\sim 0.01$ – $0.09$  ([12, 14], see also

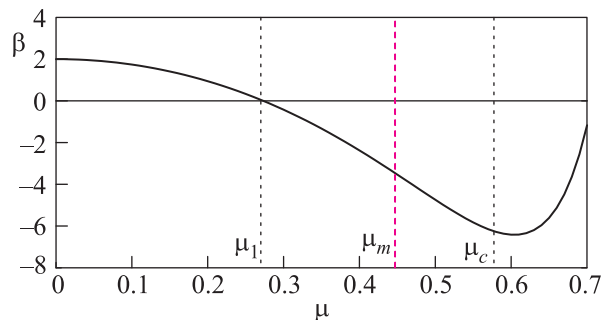


Fig. 2. Coefficient  $\beta$  of the NLS equation (19) as function of the carrier wave steepness  $\mu$  ( $\mu_1 \approx 0.274$ ,  $\mu_m \approx 0.447$ ,  $\mu_c \approx 0.577$ )

[13]). As wave steepness increases, the BFI reduces and it becomes nil at  $\mu_1$ , and breathers are suppressed. This is confirmed by recent experimental results on the Peregrine breather [15] for  $\mu \sim 0.1$ . These indicate that the “breather does not breathe”, since no return to the initial undisturbed wavetrain is observed, and its maximum amplitude is reduced in comparison to the NLS predictions.

Despite the fact that the cDZ equation is only valid for broadband waves with small values of wave steepness, the predictions beyond  $\mu_1$  may be still indicative of the trend behavior of wave dynamics near breaking. Indeed, cDZ may capture new nonlinear features that are not modelled by the NLS or higher-order Dysthe equation [21]. In particular, the BFI (and so  $\beta$ ) is negative for  $\mu > \mu_1$  and the perturbation dynamics is of defocusing type, as an indication that FPU recurrence and breathers are suppressed.

**5. Conclusions.** That NLS breathers are less likely to occur at deep water is also confirmed by an analytical solution of the excess kurtosis  $\lambda_{40}^{\text{cDZ}}$  of the local cDZ equation for weakly nonlinear waves [19]. This is smaller than the excess kurtosis  $\lambda_{40}^{\text{NLS}}$  associated with the NLS equation [22], especially as the spectrum widens. Indeed, correct to  $O(\nu^2)$  in the final-time spectral bandwidth

$$\lambda_{40}^{\text{cDZ}} = \lambda_{40}^{\text{NLS}} \left( 1 - \frac{4\sqrt{3} + \pi}{8\pi} \nu^2 \right) \approx \lambda_{40}^{\text{NLS}} (1 - 0.4\nu^2),$$

where

$$\lambda_{40}^{\text{NLS}} = \frac{\pi}{6\sqrt{3}} \frac{24\mu^2}{\nu^2}.$$

Note that wave directionality further enhances the attenuation of nonlinear focusing induced by modulational instability accelerating wave breaking. We expect the long-time evolution of a transversely unstable wavetrain of the three-dimensional (3D) version of the cDZ

equation [16] to obey the two-dimensional (2D) hyperbolic NLS equation

$$i\chi A_\xi = A_{\tau\tau} - \delta A_{\zeta\zeta} + \beta|A|^2 A - \chi q_e A, \quad (20)$$

where  $\zeta = \epsilon Y$  is the slow scale transverse to the main direction of propagation and  $\delta$  is a parameter that depends upon the wave steepness and angular spreading. Further studies on the existence of finite-blow up solutions of (20) are desirable, and they may unveil possible routes to wave breaking.

Author is grateful to Profs. Michael Banner and M. Aziz Tayfun for useful suggestions during the preparation of the manuscript. He also thanks Profs. Panayotis Kevrekidis, Taras Lakoba, and Jianke Yang for useful discussions on the subject of nonlinear waves and multiple-scale perturbation methods. Financial support is gratefully acknowledged from the National Ocean Partnership Program, through the U.S. Office of Naval Research (Grant BAA 09-012), in partnership with Ifremer.

1. T. B. Benjamin, Proc. R. Soc. (London) A **299**, 59 (1967).
2. T. B. Benjamin and J. E. Feir, J. Fluid Mech. **27**, 417 (1967).
3. P. A. E. M. Janssen, Physics of Fluids **24**, 23 (1981).
4. P. A. E. M. Janssen, J. Fluid Mech. **126**, 1 (1983).
5. E. Fermi, J. R. Pasta, and S. Ulam, Tech. Rep. Report LA-1940, Los Alamos Scientific Laboratory, 1955.
6. D. H. Peregrine, Journal of the Australian Mathematical Society Series B **25**, 16 (1983).
7. K. B. Dysthe and K. Trulsen, Physica Scripta T **82**, 48 (1999).
8. A. R. Osborne, M. Onorato, and M. Serio, Phys. Lett. A **275**(5,6), 386 (2000).
9. P. A. E. M. Janssen, Journal of Physical Oceanography **33**(4), 863 (2003).
10. C. Kharif and E. Pelinovsky, Eur. J. Mech. B/Fluids **22**, 603 (2003).
11. K. B. Dysthe, H. E. Krogsted, and P. Müller, Annual Review Fluid Mech. **40**, 287 (2008).
12. A. Chabchoub, N. Hoffmann, M. Onorato, and N. Akhmediev, Phys. Rev. X **2**, 011015 (2012).
13. A. Chabchoub, N. Hoffmann, and N. Akhmediev, Phys. Rev. Lett. **106**, 204502 (2011).
14. A. Slunyaev, E. Pelinovsky, A. Sergeeva et al., Phys. Rev. E **88**, 012909 (2013).
15. L. Shemer and S. H. Alperovich, Physics of Fluids **25**, 051701 (2013).
16. A. I. Dyachenko and V. E. Zakharov, JETP Lett. **93**(12), 701 (2011).

17. F. Fedele and D. Dutykh, *J. Fluid Mech.* **712**, 646 (2012).
18. D. R. Crawford, B. M. Lake, P. G. Saffmann, and H. C. Yuen, *J. Fluid Mech.* **105**, 177 (1981).
19. F. Fedele, <http://arxiv.org/abs/1309.0668> (2013).
20. C. M. Schober, *European Journal of Mechanics – B/Fluids* **25**(5), 602 (2006).
21. K. B. Dysthe, *Proc. R. Soc. Lond. A* **369**, 105 (1979).
22. N. Mori and P. A. E. M. Janssen, *Journal of Physical Oceanography* **36**(7), 1471 (2006).